fortune Journals

Research Article

JOURNAL OF ANALYTICAL TECHNIQUES AND RESEARCH

ISSN: 2687-8038

Plasmon-Induced Flexibility and Refractive Index Measurement in A Sensor Designed by a Cavity, Two Rings, Two Teeth and Two Plasmonic Waveguides

Hamid Abbasi*

Abstract

In this research, we design a plasmonic refractive index sensor and examine it numerically, using transparency, refractive index, sensitivity, FOM fit shape and Q quality factor, to optimize and improve performance quality. We will be. To design the structure of this sensor, we use two plasmonic waveguides, a cavity, two rings and two teeth. The resonant wavelengths and refractive index of the resonators are investigated and simulated by the finite difference time domain (FDTD) method, and we draw the obtained diagrams using MATLAB software. After completing the sensor design, due to the fact that the amplifiers are very sensitive to changes in the refractive index, so by changing the refractive index and changing the dimensions of the structure, we can weaken or strengthen the passage coefficient in the resonant modes. These plasmonic sensors with a simple frame and high optical resolution can be used to measure refractive index in the medical, chemical and food industries.

Keywords: Photonic; Plasmonic; Surface Plasmons; Waveguide; Resonators; Optic.

Introduction

Surface plasmon polaritons (SPPs) have been studied extensively recently due to the fact that they confine light at nanoscale dimensions [1]. As a result of these unique features, SPPs are used in many structures such as filters [2], optical demultiplexers, bio-sensors [3-36], logic gates and etc. The metal–insulator-metal (MIM) optical waveguide is used extensively for design of many plasmonic devices due to its ability to confine light within a small area and its compatibility with electronic platforms [37-46]. In addition, having a simple design procedure makes it one of the most favorable structures. Consequently, a diversity of MIM plasmonic devices have been designed and implemented. Some of them are optical filters, sensors, coulpers, slow light devices, splitters and all-optical switches. A good refractive index sensor needs to have a good sensitivity (S) and a high figure of merit (FOM). Increasing the device size usually increases the sensitivity, but larger structures have higher full width half maximum, which leads to a reduction of FOM. Many criteria can be used to implement refractive index sensors, but plasmonic sensors are more suitable for integrated circuits due to their very small size (nanometers). Recently, various types of plasmonic sensors have been designed and manufactured. Among them, plasmonic refractive index sensors require high sensitivity and resolution. Conventional plasmonic sensors consist of a MIM waveguide with a cavity. Such cavities can have a variety of geometries such as tooth-shaped, disc-shaped, ring-shaped, and so on. In this paper, we propose a MIM plasmonic sensor with two rings and a cavity and two teeth.

Affiliation:
University of Mazandaran, Iran.

***Corresponding author:**
Hamid Abbasi, University of Mazandaran, Iran.

Citation: Hamid Abbasi. Plasmon-Induced Flexibility and Refractive Index Measurement in A Sensor Designed by a Cavity, Two Rings, Two Teeth and Two Plasmonic Waveguides. Journal of Analytical Techniques and Research 5 (2023): 16-20.

Received: September 27, 2023
Accepted: October 18, 2023
Published: October 30, 2023

Abbasi H., J Anal Tech Res 2023
DOI:10.26502/jatr.36

To simulate the sensor, the two-dimensional finite difference time domain (FDTD) method with a uniform mesh size of 8 nm has been used. The boundary condition for all directions is selected as the perfectly matched layer (PML).

Structural model and theory analysis

There are many structures for designing optical sensors. These optical sensors usually include amplifiers and waveguides. Each waveguide with any geometric shape has the ability to transmit waves and can limit their energy in one and two dimensions. The proposed structure is shown in Figure 1, which includes two waveguides and a cavity, and two rings and two teeth. The input wave goes from the left waveguide to the structure and after passing through them goes to the output waveguide. The width of the two waveguides is w1 = 50 nm. The middle ring is located in the middle of two waveguides that have an inner radius of r1 = 90 nm and an outer radius of R1 = 133 nm, which is located at a distance of 19 nm from the two waveguides. The two teeth are connected to the middle ring, which has a length of 40 nm and a height of 20 nm. A ring is located at the bottom of the right waveguide and has an inner radius of r1 = 91 nm and an outer radius of R1 = 126 nm. The cavity also has a length of L = 80 nm and a height of W2 = 200 nm. The lower ring is attached to the waveguide and the cavity and the distance from the cavity to the waveguide is 55 nm. Pin and Pout are the monitors for measuring the input and output waves, respectively, and the transmission is calculated by T = Pout / Pin.

As shown in the 2D image, the green and white areas represent silver and air, respectively. The air permittivity is set to ε = 1 and the silver permittivity is used using the greeting model as follows:

$$\varepsilon(\omega) = \varepsilon_\infty - \frac{\omega_p^2}{\omega^2 + i\nu\omega} \quad (1)$$

Here c∞ gives the medium constant for the infinite frequency, ωp refers to bulk frequency for plasma, γ means damping frequency for electron oscillation, and ω shows incident light angular frequency. The parameters for silver are c∞ = 1, ωp =1.37 × 1016 Hz, and γ = 3.21 × 1013 Hz. Only TM mode is available in the structure. According to Figure 1, the TM wave, which is used for SPP excited waves, starts propagating from the left waveguide and propagates in the waveguide, and its intensity decreases as it gets closer to the output port. After distributing the field at the resonant frequency of the simulated structure, each amplifier reflects a certain amount of input wave.

Fracture coefficient simulation and measurement methods

The resonant behavior of the proposed structure is examined numerically and theoretically. In the numerical approach, we use the time domain finite difference (FDTD) simulation method with perfectly matched layer boundary conditions (PML) because this method effectively reduces the numerical reflection. The uniform mesh size is 8 nm. First, to measure the performance of the sensor and increase its quality, we must change its refractive index. This is done in the wavelength range of 400 to 1500 nm and the refractive index of the middle ring will change in steps of 0.01 from 1.15 to 1.2 nm. An electromagnetic field is generated by the excitation of a sensing element using light generated by SP that is concentrated on the metal surface. The refractive index of the MIM changes when the material under contact contacts the sensor. SPs are very sensitive to changes in refractive index in the vicinity of the surface. The reason we have only changed the refractive index of one ring and the refractive index of other amplifiers remains the same is to achieve a better result and a stronger sensor design. The transmission spectrum from the sensor device is shown in Figure 2.

After comparing the wavelengths using the refractive index change and plotting the transmission spectrum, we must obtain the three criteria of sensitivity S and the shape of the FOM and the quality factor Q. With this, we create

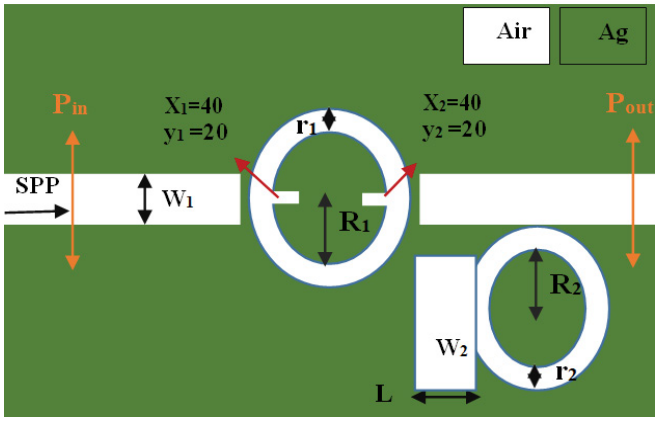

Figure 1: Two-dimensional image of a plasmonic sensor

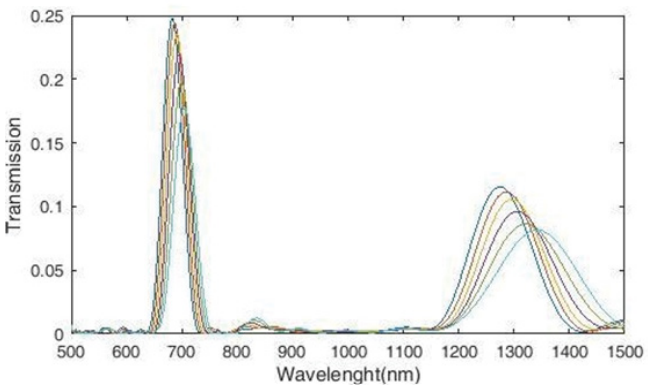

Figure 2: Transmission spectra of plasmonic refractive index sensor

Citation: Hamid Abbasi. Plasmon-Induced Flexibility and Refractive Index Measurement in A Sensor Designed by a Cavity, Two Rings, Two Teeth and Two Plasmonic Waveguides. Journal of Analytical Techniques and Research 5 (2023): 16-20.

Abbasi H., J Anal Tech Res 2023
DOI:10.26502/jatr.36

a technology map to define the standard and development process of optical refractive index sensors. Sensitivity S defines the ratio of the output wavelength change of the sensor to the refractive index changes and is obtained from the following relation:

$$S = \Delta \lambda / \Delta n \text{ (nm / RIU)} \quad (2)$$

We see the diagram of the plasmonic sensitivity coefficient in Figure 3, which according to the figure, has the highest sensitivity for the refractive index n = 1.2 (in mode2) which is equal to 2359 nm / RIU and the lowest value for the refractive index n = 1.16 (in mode1) Which is equal to 314.1 nm / RIU.

The next item is the figure of merit (FOM), which determines the sensitivity of the SRI to the resonance width curve (FWHM) and how accurately the minimum resonance can be measured. FOM is calculated as follows:

$$FOM = SRI / FWHM \quad (3)$$

We see the diagram of the figure of merit (FOM) in Figure 4, which according to the figure has the highest value for the refractive index n = 1.18 (in mode1) which is equal to 15.03 and the lowest value for the refractive index n = 1.12 (in mode1) which is equal to With 7.354.

And the last case is the quality factor Q, which is obtained from the following equation:

$$Q = \lambda res / FWHM \quad (4)$$

We see the quality factor Q diagram in Figure 5.

According to the figure, the highest value of quality factor Q is for refractive index n = 1.17 (in mode1) which is equal to 16.56 and the lowest value for refractive index is n = 1.19 (in mode2) which is equal to 7.379. These three factors (S and FOM sensitivity and Q quality factor) and their numerical values showed that this sensor has good performance and quality and has a higher sensitivity compared to similar articles.

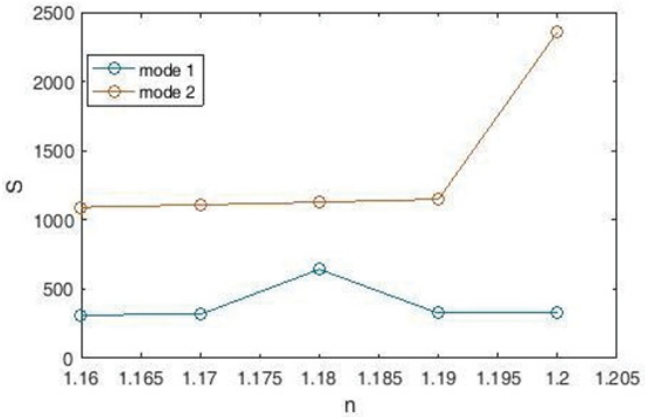

Figure 3: Plasmonic sensor sensitivity coefficient diagram Resonance wavelength versus refractive index analysis.

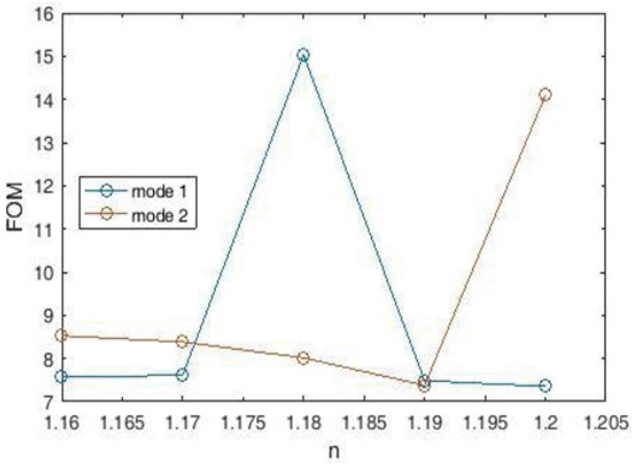

Figure 4: Plasmonic sensor FOM diagram.

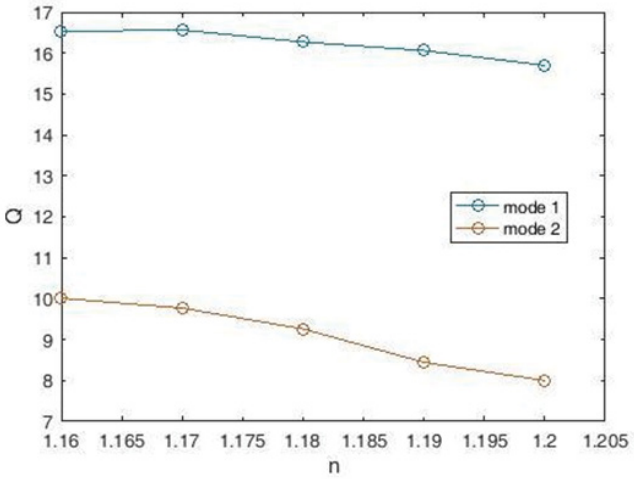

Figure 5: Quality factor diagram of Q plasmonic sensor.

Conclusion

In this paper, a very high resolution refractive index optical sensor is presented. It is based on plasmonic conductors of metal-metal insulation. The structure is numerically simulated using the finite difference time domain method. The proposed structure is thought to consist of two plasmonic waveguides, a cavity, two rings and two teeth. This sensor provides a sensitivity of 2359 nm / RIU and a maximum rating of 15.0316 RIU-1 (FOM). Due to its high resolution resolution, this sensor can easily change 0.01% in the analytic refractive index for the index in the range of 1.15-1.2.

Competing Interest

The authors declare no conflicts of interest.

References

1. Ebbesen, Thomas W, A Dereux, et al. Surface plasmon subwavelength optics. Nature 424 (2003): 824-830.

2. Wu W. Ultra-high resolution filter and optical field modulator based on a surface plasmon polariton. Optics Letters 41 (2016): 2310.
3. Chen L. Numerical analysis of a near-infrared plasmonic refractive index sensor with high figure of merit based on a fillet cavity. Optics Express 24 (2016): 9975.
4. Tong L. Recent advances in plasmonic sensors. Sensors 14 (2014): 7959.
5. Y Shen, JH Zhou, TR Liu, et al, Plasmonic gold mushroom arrays with refractive index sensing figures of merit approaching the theoretical limit. Nat. Commun 4 (2013): 2381.
6. Srivastava, Triranjita, R Das, et al. Highly Sensitive Plasmonic Temperature Sensor Based on Photonic Crystal Surface Plasmon Waveguide. Plasmonics 8 (2013): 515-521.
7. Maisonneuve M. Phase sensitive sensor on plasmonic nanograting structures. Optics Express 19 (2011): 26318-26324.
8. Elsayed, Mohamed Y, Y Ismail, et al. Semiconductor plasmonic gas sensor using on-chip infrared spectroscopy. Applied Physics 123 (2017): 113.
9. Cen C, Lin H, Huang J, et al. A Tunable Plasmonic Refractive Index Sensor with Nanoring-Strip Graphene Arrays. Sensors 18 (2018): 4489.
10. Cheng F, Yang X, Gao J. Enhancing intensity and refractive index sensing capability with infrared plasmonic perfect absorbers. Opt Lett 39 (2014): 3185-3188.
11. Cheng L, Wang Z, He X, et al. Plasmonic nanosensor based on multiple independently tunable Fano resonances. Beilstein J Nanotechnol 10 (2019): 2527-2537.
12. Chou Chao CT, Chou Chau YF, Huang HJ, et al. Highly Sensitive and Tunable Plasmonic Sensor Based on a Nanoring Resonator with Silver Nanorods. Nanomaterials (Basel) 10 (2020): 1399.
13. Di Wu, Jinping Tian, Lu Li, et al. Plasmon induced transparency and refractive index sensing in a new type of graphene-based plasmonic waveguide. Optics Communications (2018).
14. E. Haque, S Mahmuda, MA Hossain, et al. "Highly Sensitive Dual-Core PCF Based Plasmonic Refractive Index Sensor for Low Refractive Index Detection," in IEEE Photonics Journal 11 (2019): 1-10.
15. El Shamy RS, Khalil D, Swillam MA. Mid Infrared Optical Gas Sensor Using Plasmonic Mach-Zehnder Interferometer. Sci Rep 10 (2020): 1293.
16. 168-Esfahani Monfared Y. Overview of Recent Advances in the Design of Plasmonic Fiber-Optic Biosensors. Biosensors 10 (2020): 77.
17. Gryga M, Ciprian D, Hlubina P. Bloch Surface Wave Resonance Based Sensors as an Alternative to Surface Plasmon Resonance Sensors. Sensors 20 (2020): 5119.
18. ghiasi M, Mehrzad H, Mohajerani E. Sensor based on plasmonic absorption of island metal films, varying refractive index of the surrounding environment (2017).
19. Gomez-Cardona N, Reyes-Vera E, Torres P. High Sensitivity Refractive Index Sensor Based on the Excitation of Long-Range Surface Plasmon Polaritons in H-Shaped Optical Fiber. Sensors 20 (2020): 2111.
20. Kanso M, Cuenot S and Louarn G. Sensitivity of Optical Fiber Sensor Based on Surface Plasmon Resonance: Modeling and Experiments. Plasmonics 3 (2008): 49-57.
21. MA Butt, SN Khonina and NL Kazanskiy. "Plasmonic refractive index sensor based on M-I-M square ring resonator," International Conference on Computing, Electronic and Electrical Engineering (ICE Cube) (2018).
22. Mayer KM and Hafner JH. Localized surface plasmon resonance sensors. Chemical reviews 6 (2011): 3828-3857.
23. Mohammad Reza Rakhshani. Wide-angle perfect absorber using a 3D nanorod metasurface as a plasmonic sensor for detecting cancerous cells and its tuning with a graphene layer.Photonics and Nanostructures -Fundamentals and Applications.photonics 30 (2022): 10387-10399.
24. Zhang Z, Yang J, He X, et al. Plasmonic Refractive Index Sensor with High Figure of Merit Based on Concentric-Rings Resonator. Sensors 18 (2018): 116.
25. Nguyen HH, Park J, Kang S, et al. Surface plasmon resonance: a versatile technique for biosensor applications. Sensors 15 (2015): 10481-10510.
26. Rabiul Al Mahmud, Md Omar Faruque, Rakibul Hasan Sagor. A highly sensitive plasmonic refractive index sensor based on triangular resonator.Optics Communications 483 (2021): 126634.
27. Rahmatiyar M, Danaie M and Afsahi M. Employment of cascaded coupled resonators for resolution enhancement in plasmonic refractive index sensors. Opt Quant Electron 52 (2020): 153.
28. Rashed AR, Gudulluoglu B, Yun HW, et al. Highly-SensitiveRefractive Index Sensing by Near-infrared Metatronic Nanocircuits. Sci Rep 8 (2018).
29. RM Piragash Kumar, A Venkatesh, VHS Moorthy. Nanopits based novel hybrid plasmonic nanosensor fabricated by a facile nanofabrication technique for biosensing, Materials Research Express 6 (2019): 1-19.

Abbasi H., J Anal Tech Res 2023
DOI:10.26502/jatr.36

30. Somayyeh Asgari, Siavash Pooretemad, Nosrat Granpayeh. Plasmonic refractive index sensor based on a double concentric square ring resonator and stub. Photonics and Nanostructures - Fundamentals and Applications 42 (2020): 100857.

31. Takashima Y, Haraguchi M, Naoi Y. GaN-Based High-Contrast Grating for Refractive Index Sensor Operating Blue–Violet Wavelength Region. Sensors 20 (2020): 4444.

32. Wang X, Wu X, Zhu J, et al. Theoretical Investigation of a Highly Sensitive Refractive- Index Sensor Based on TM0 Waveguide Mode Resonance Excited in an Asymmetric Metal-Cladding Dielectric Waveguide Structure. Sensors 19 (2019): 1187.

33. Wenger Tobias, Viola Giovanni, Kinaret, et al. High-sensitivity plasmonic refractive index sensing using grapheme. 2D Materials 4 (2017).

34. Xiling Shi, Lianjun Ma, Zhidong Zhang, et al. Dual Fano resonance control and refractive index sensors based on a plasmonic waveguide-coupled resonator system. Optics Communications 427 (2018): 326-330.

35. Yang X, Hua E, Su H, et al. A Nanostructure with Defect Based on Fano Resonance for Application on Refractive-Index and Temperature Sensing. Sensors (Basel) 20 (2020): 4125.

36. Yangyang Chen, Jinchuan Liu, Zhenchuan Yang, et al. (2019). Optical biosensors based on refractometric sensing schemes: A review, Biosensors and Bioelectronics 144 (2019): 111693.

37. Maier, Stefan A. Plasmonics: Fundamentals and Applications. Springer Berlin 52 (2014): 49-74.

38. Shu, Changgan. The sensing characteristics of plasmonic waveguide with a ring resonator. Optics Express 22 (2014): 7669-7677.

39. Yan, Shu Bin. A Refractive Index Sensor Based on a Metal-Insulator-Metal Waveguide-Coupled Ring Resonator. Sensors 15 (2015): 29183-29191.

40. Huang, Ye Xiong. A plasmonic refractive index sensor based on a MIM waveguide with a side-coupled nanodisk resonator. IEEE, International Conference on Embedded and Real-Time Computing Systems and Applications IEEE (2014): 1-5.

41. Wu, Tiesheng. A nanometeric temperature sensor based on plasmonic waveguide with an ethanol-sealed rectangular cavity. Optics Communications 339 (2015): 1-6.

42. Tang, Y. Refractive Index Sensor Based on Fano Resonances in Metal-Insulator-Metal Waveguides Coupled with Resonators. Sensors 17 (2017): 784.

43. Zhang, Zhidong. Fano Resonance Based on Metal-Insulator-Metal Waveguide-Coupled Double Rectangular Cavities for Plasmonic Nanosensors. Sensors 16 (2016): 642.

44. Zafar, Rukhsar, and M. Salim. Enhanced Figure of Merit in Fano Resonance-Based Plasmonic Refractive Index Sensor. IEEE Sensors Journal 15 (2015): 6313-6317.

45. Zhao X, Z Zhang and S Yan. Tunable Fano Resonance in Asymmetric MIM Waveguide Structure. Sensors 17 (2017): 7.

46. Chen, Jianjun. Coupled-Resonator-Induced Fano Resonances for Plasmonic Sensing with Ultra-High Figure of Merits. Plasmonics 8 (2013): 1627-1631.